SYNTHESIS OF NOVEL ALL-DIELECTRIC GRATING FILTERS USING GENETIC ALGORITHMS

Cinzia Zuffada, Tom Cwik and Christopher Ditchman

Jet Propulsion Laboratory

California Institute of Technology

Pasadena, CA 91109

ABSTRACT

The feasibility of novel all-dielectric waveguide grating filters is demonstrated, using a genetic algorithm to solve for material dielectric constants and geometric boundaries separating homogeneous regions of the periodic cell. In particular, genetic algorithms show that simple geometries, not previously reported, utilizing a small number of layers and/or gratings, can be found to yield bandpass or stopband filters with user defined linewidth. The evaluation of the fitness of a candidate design entails the solution of an integral equation for the electric field in the cell using the method of moments. Our implementation is made efficient by using only very few design frequency points, and accurately approximating a given filter transfer function by a quotient of polynomials as a function of frequency. Additionally, the problem impedance matrices are conveniently represented as the product of a material independent matrix and a vector of dielectric constants, thus allowing us to fill the matrices only once. Our code has been parallelized for the Cray T3D, to take advantage of the intrinsic parallelization efficiencies offered by genetic algorithms. Solutions are illustrated for a very narrowband single grating transmission filter, and a relatively broadband double grating reflection filter. Additionally, a solution for a five homogeneous layers Fabry-Perot filter is also presented.

1. Introduction

This work is concerned with the synthesis of inhomogeneous, all dielectric (lossless) periodic structures which act as filters. The design of electromagnetic components, in general, involves finding the values of the relevant parameters which ensure that the structure performs in accordance with specified design criteria. The particular type of design described here can be thought of as an inverse-source problem, since it entails finding a distribution of sources which produce fields (or quantities derived from them) of given characteristics. Electromagnetic sources (electric and magnetic current densities) in a volume are related to the outside fields by a well known linear integral equation. Additionally, the sources are related to the fields inside the volume by a constitutive equation, involving the material properties. Then, the relationship linking the fields outside the source region to those inside is non-linear, in terms of material properties such as permittivity, permeability and conductivity. Dielectric filters made as stacks of inhomogeneous gratings and layers of materials have been used in optical technology for some time, but are not common at microwave frequencies. The problem is then finding the periodic cell's geometric configuration and permittivity values which correspond to a specified reflectivity/transmittivity response.

This type of design problem shares some of the formalism with that of the identification/location of dielectric objects given their scattered fields, in that they are both non-linear inverse problems described by the same integral equations. Some approaches to solving the reconstruction problem have been proposed [1], [2] which suggest a useful strategy also applicable in part to the design case. Specifically, the solution of the non-linear inverse problem is cast as a combination of two linear steps, by explicitly introducing the electromagnetic sources in the computational volume as a set of unknowns in addition to the material unknowns. This allows to solve for material parameters and electric fields in the source volume which are consistent with Maxwell's equations. Solutions are obtained iteratively by either decoupling the two steps in [1] or by keeping them coupled in [2].

Irrespective of the specific solution method, this approach involves a potentially large number of unknowns, particularly when many frequencies/illumination angles are of interest, which is the case in design. We introduce a simplification in the iterative scheme by first inverting for the permittivity only in the minimization of a cost function and then, given the materials, by finding the corresponding electric fields through direct solution of the integral equation in the source volume. The sources thus computed are used to generate the far fields and the synthesized filter response. The cost function is obtained by calculating the deviation between the synthesized value of reflectivity/transmittivity and the desired one. Solution geometries for the periodic cell are sought as gratings (ensembles of columns of different heights and/or widths), or combinations of homogeneous layers of different dielectric materials and gratings. Hence the explicit unknowns of the inversion step are the material permittivities and the relative boundaries separating homogeneous parcels of the periodic cell.

The inversion step to compute materials and geometric boundaries is performed using the genetic algorithm package PGAPACK [3]. Several advantages are offered by genetic algorithms (GA) over gradient-based or other methods, for electromagnetic design problems where the solution space has many extrema. Some applications reported in the literature include the design of thinned phased-arrays [4], of multilayer radar absorbers [5], of multilayer optical filters [6], of loaded antennas [7], [8], and of MMIC component shapes [9]. In particular, the ability of genetic algorithms to sample the parameter space globally not only avoids the common pitfalls of local minimization algorithms, but holds the promise of finding novel solutions perhaps not thought to exist. This, in fact, has been the primary objective of this work; specifically, the investigation and evaluation of dielectric filter solutions whose geometry is simpler or smaller than existing designs, and the understanding of the ensuing trends in required numbers and values of materials and their configurations.

It has been remarked that genetic algorithms carry a considerable computational cost. Naturally the most expensive part of the computational cycle is the 'forward module' that performs the evaluation of a candidate solution to determine its fitness. In our case this consists of solving a set of integral equations for the electric fields in the cell, one for each design frequency/illumination angle. Although the impedance matrix depends on the solution vector of materials and boundaries candidates, it can be formed as a product of a solution-independent matrix and a vector. This procedure allows us to fill the set of frequency-dependent impedance matrices only once. Additionally, the number of design frequencies at which the integral equations are actually solved is a small set of values within the frequency range of the desired filter response. The reduction is afforded by approximating the desired filter response by a quotient of frequency dependent polynomials, through the procedure of transfer function parameter estimation described in [10]. Furthermore, full advantage has been taken of the parallel implementation of PGAPACK for the Cray T3D. The parallelization scheme used for the genetic algorithm is an intuitive, simple master-slave configuration, where the expensive evaluation cycles are distributed among the processors.

Section 2 describes the electromagnetic scattering from a two-dimensional inhomogeneous dielectric periodic structure, which consitutes the 'forward module' of our inversion scheme; section 3 highlights some of the relevant features of the specific GA solver used in our work. Section 4 focuses on the design of dielectric waveguide-grating filters and emphasises the role of our inverse approach in finding novel solutions; section 5 presents and discusses numerical results for three different types of filters designed with our code.

2. Formulation of the Forward Scattering from a Dielectric Grating

At every step we evaluate the scattering from a candidate solution for a dielectric grating according to the formulation described in the following. Figure 1a shows the geometry of a dielectric grating, periodic in the x dimension, infinite in y, and having a

thickness $t(x)$ variable over the cell. The cell material is characterized by complex permittivity and permeability. The polarization with the electric field parallel to the strip will be considered (E - polarization); a formulation for the perpendicular polarization can be similarly developed. To properly pose the scattering problem for a periodic structure, the excitation field must be a function with constant amplitude and linear phase. The incident field is defined as [11]

$$E^i(x,z) = E_0 \psi_0(x)\ e^{jk_{z_0} z} \tag{1}$$

where

$$\psi_m(x) = \frac{1}{\sqrt{T_x}} e^{jk_{x_m} x} \tag{2}$$

and

$$k_{x_m} = \frac{2\pi}{T_x} m + k_{x_0}, \quad k_{x_0} = k \sin\theta^i$$

$$k_{z_m} = \begin{Bmatrix} \sqrt{k^2 - k_{x_m}^2}\ , & k \geq k_{x_m} \\ -j\sqrt{k_{x_m}^2 - k^2}\ , & k \leq k_{x_m} \end{Bmatrix}$$

and the $e^{j\omega t}$ time convention is used. Using the electric field integral equation, the unknown induced current J(ρ) is found, at each design frequency/illumination angle, from

$$E^i(\rho) = \frac{1}{j\omega\varepsilon_0 \chi(\rho)} J(\rho) - E^s(\rho) \tag{3}$$

where all components are y directed, and χ is the contrast function

$$\chi(\rho) = \varepsilon_r(\rho) - 1$$

The scattered field is found from integrating the induced currents over the grating

$$E^s(x,z) = \frac{-\omega}{4} \int_0^{T_x} \int_0^{t(x)} \mu(x',z') J(x',z') G_p(x,z|x',z') dx', dz' \tag{4}$$

where

$$G_p(x,z|x',z') = \frac{1}{4j} \sum_{m=-\infty}^{\infty} H_0^{(2)}(k\sqrt{(x-x'-mT_x)^2 + (z-z')^2}) \; e^{jkx_0 mT_x}$$

is the two-dimensional periodic Green's function – the outgoing Hankel function of order zero – representing the field due to source points within each cell [12]. Using this periodic spatial Green's function, the integration area is then over one periodic cell. Equation (4) contains an integrable singularity, occurring as the source and observation points are made to coincide. The Appendix outlines a method for isolating this singular point and performing the integration in an efficient manner. The result is

$$E^s(x,z) = \int_0^{T_x} dx' \int_0^{t} dz' J(x',z') \left[Z_m^P(x,z|x',z') - Z_m^P(x,z|x',z'+\delta) \right]$$

$$+ \sum_m \tilde{Z}_m \tilde{I}_m^{\pm} \psi_m(x) \; e^{\mp k z_m (z+\delta)} \tag{5}$$

where the various terms are defined in the Appendix.

The method of moments is used to solve the above integral equation. The numerical solution of (3) is found by first discretizing the current over a periodic cell in a pulse basis set

$$J(x,z) = \sum_{p'=1}^{P} \sum_{q'=1}^{Q} C_{p'q'} \pi_{p'}(x) \pi_{q'}(z), \quad P'x\,Q' = P'Q' \tag{6}$$

where the pulse is defined as

$$\pi_p(u) = \begin{Bmatrix} 1, & (p-1)\Delta u < u < p\Delta u \\ 0, & elsewhere \end{Bmatrix}$$

In our method of moments procedure point matching is used, with the testing functions being

$$T_{pq}(x,z) = \delta[x - (p - \frac{1}{2})\Delta x]\ \ \delta[z - (q - \frac{1}{2})\Delta z] \tag{7}$$

The matrix system for the unknown coefficients C is then

$$\left\langle E^i, T_{pq} \right\rangle = \sum_{p'q'} C_{p'q'} \left\langle \ \frac{1}{j\omega\varepsilon_0\chi} \pi_{p'}\pi_{q'}, T_{pq} \ \right\rangle$$

$$- \sum_{p'q'} \left[\left\langle E^{ss}(x,z), T_{pq} \right\rangle + \left\langle E^{sn}(x,z), T_{pq} \right\rangle \right] \quad pq = 1,2,...P'Q' \tag{8}$$

where the inner product is defined as

$$\langle f, g \rangle = \int_0^{T_x} dx \int_0^{t} dz\, fg^*$$

The matrix of (8) depends on the materials through the contrast χ. However, it can be represented as a product of a material-independent matrix times the vector of the contrasts at each discretization cell. Therefore, the basic matrix is filled only once for each

design frequency, and it is simply updated at each iteration step by multiplication with the current vector of contrasts. It seems that there is one independent contrast value for each discretization cell used in our method of moments. In reality, we constrain the grating periodic cell to be composed of a number of regions with different materials, separated by boundaries, and arranged in a combination of homogeneous horizontal layers and/or strips with χ varying along the x and z directions, as illustrated in Figures 1b-c. Then the set of inversion parameters for the GA, i.e. the different values for χ and boundary locations along x and z, is much smaller than the number of discretization cells. A mapping algorithm transforms this reduced parameter set for a candidate solution to the full vector of contrasts at each discretization cell.

Assuming that only the dominant (m = 0) mode is propagating, the reflection and transmission coefficients are found from evaluating the total field at z >> t, and z <<0 respectively,

$$R = \frac{-\omega}{4E_0}\frac{1}{2jk_{z_0}}\int_0^t dz'\mu\tilde{J}_0(z')\ e^{jk_{z_0}z'} \tag{9a}$$

$$T = 1 - \frac{\omega}{4E_0}\frac{1}{2jk_{z_0}}\int_0^t dz'\mu\tilde{J}_0(z')\, e^{-jk_{z_0}z'} \tag{9b}$$

where the transform of the current is given in the Appendix.

In designing a filter the desired behavior of R and T *(RR* or TT*)* within a continuous range of frequencies is often specified; since the coefficients of the current are frequency dependent it would appear that to evaluate the response of a candidate many method of moments solutions of (5) must be calculated. However, any prescribed filter response must satisfy the condition of realizability. It is well known from classical lumped parameter filter design that realizability requires that the insertion loss, as a function of frequency, be representabable as the ratio of two polynomials of even powers of

frequency. In our particular problem this requirement is found to apply approximately to the filter transmittivity and/or reflectivity. Then the problem is reduced to representing the desired filter response by a quotient of polynomials, working with a set of prescribed values sufficient to determine the unknown coefficients. As discussed in [10], the general representation for a magnitude-squared network transfer function with poles and zeroes is given by

$$|F(\omega_i)|^2 = \frac{\sum_{j=0}^{N-1} B_j(\omega_i)^{2j}}{\sum_{j=0}^{N} A_j(\omega_i)^{2j}} + \sum_{j=0}^{K} C_j(\omega_i)^{2j} \qquad (10)$$

where the quantity on the left-hand-side is either RR^* or TT^*. Equation (10) can easily be turned into a system of equations in the 2xN+K unknowns A_j, B_j and C_j. Hence the solution of (5) is calculated only at 2xN+K design frequencies, and the correspondent values for (9a) or (9b) are used to solve for (10). The polynomial approximation of (9a) or (9b) are then obtained at all frequencies of interest, and used in the evaluation of the residual.

3. PGAPACK Parallel Genetic Algorithm

The general properties of genetic algorithms are described very extensively in the literature (see, for example, [13]) and here we summarize only the most important features of the specific library used in our work. PGAPACK is a parallel genetic algorithm library developed at Argonne National Laboratory by D. Levine [3]. Both serial and parallel versions are available, for a large number of computer systems, including the Cray T3D, using MPI system libraries. The low-level routines are written in C, but interface (wrappers) routines are available which allow PGAPACK to be used in a FORTRAN code. For simple problems, or limited user involvement, a single high level call to the library is available. More user control can be achieved by calling the genetic algorithm lower level

functions explicitly, in which case many parameters affecting the mechanisms of selection, recombination and fitness evaluation can be adjusted. We have chosen a flexible, customized usage in our work, which included writing some additional low level routines. Several data types are admissible to represent the string of unknowns called 'gene'; we have chosen real encoding, whereby each unknown is represented by one real number whose value can vary continuosly within a predefined range. Hence the solutions are not limited to the discrete approximations associated with a binary representation. We find real encoding very appealing also because the meaning of the operations of crossover and mutation are more transparent, and we believe more effective, than for binary encoding. To illustrate the point on a simple example, we have simulated the application of a crossover and a mutation operations to a real encoded gene contrasted to a binary encoded gene in Figure 2. (Note that the two representations are not meant to describe the same numbers). It is assumed that there are four variables and that three bits have been chosen to represent each of them in the binary approximation; by contrast a full real number is used to represent an allele in real encoded genes. A two-point crossover has been chosen in both cases. In either case the crossover operation generates new strings by combining portions of two existing strings, broken at one or more points. While in a binary representation the bit sequence representing one variable can be broken by the crossover operation at any point, as illustrated in (α) on the left of Figure 2, in a real encoding the full value of a variable is always preserved, as seen in (α) on the right of Figure 2. Crossover then simply rearranges the sequence of candidate values, and then mutation changes them. Note also that the mutation operation acquires a more versatile meaning, and is not just the flipping of a bit in the string. Instead, an allele is mutated by modifying its value according to some algorithms; for example by a percentage of the current value, chosen probabilistically within a range (compare, for example, (β) on the left and right of Figure 2). One can see that, with real encoding, crossover is the most important operation during the early generations, when the gross features of a good solution are evolved. Later on

mutation becomes the critical mechanism which allows the fine features of the solution to emerge. In addition to the types of encoding described so far, PGAPACK allows the user to define custom data types, which implies writing a set of custom functions to perform the operations which are data-type dependent. This facility is very useful for problems requiring a mixed type of variable encoding.

4. An Application: Guided-Mode Resonance Filters

It has been demonstrated that planar dielectric layer diffraction gratings exbibit sharp resonances due to the coupling of exterior evanescent diffractive fields to the leaky modes of dielectric waveguides. In these cases efficient switching of energy between (nearly) totally reflected zero-order mode and (nearly) totally transmitted zero-order mode is achieved with proper choice of the cell size. Such property leads to the possibility of filter designs whose arbitrarily narrow linewidths can be controlled by the choice of modulation amplitude and mode confinement. In optics the guided-mode resonance effect has been combined with classical antireflection properties of thin film structures, leading to the design of symmetric reflection filters, with low sidebands over wavelength ranges related to the number of films used and their dielectric constants [14]. Recently, a combination of guided-mode resonance and high-reflection layer design has been demontrated to yield transmission bandpass filters [15]. A reflection filter of this type has also been demonstrated in the microwave region [16]. In the present paper we investigate the possibility of finding new types of waveguide-grating filter solutions in the microwave region. In the above studies 'forward scattering' analysis techniques were used to obtain the filter response, starting from a set of user specified filter parameters and relying on known properties of anti-reflection (half-wavelength) or high-reflection (quarter wavelength) homogeneous layers/gratings for reflection and transmission filters, respectively. By contrast, here we start from a desired filter response and determine the grating/layer configuration and dielectric constants of the solution, without constraining the thicknesses to be a specified fraction of the resonance wavelength. This approach is

particularly appealing in the microwave where the traditional approach used in optics would yield solutions which are too thick for practical use. At the same time the potential reduction in size can be beneficial in optics too, since thinner filters have a wider range of application.

Some important issues can be explored with our inverse approach. The first relates to the shape of the resonance response of the filter; in particular, we have investigated the possibility of synthesizing a transmission response described by a Lorentzian lineshape with controllable linewidth, to achieve a very narrow band. On the other hand, we have also searched for solutions whose reflection response follows a given Butterworth curve, to demonstrate that broadbanded response and sharp cutoff are also obtainable with these type of structures. A second issue concerns the actual number and configuration of gratings/layers required; specifically, we have been looking for the 'simplest' solutions, i.e. those which involve only one grating, if possible. In particular, we have also investigated the possibility of using more than two materials to make one grating, to achieve symmetric responses, exhibiting a sharp resonance and low side-bands. We have seen that there is a trade-off between the values of the dielectric constants (resulting in the modulation) and the thickness of the periodic cell. Since it is our interest to examine the possibility of designs which might not be known to exist, we have not restricted the choice of dielectric constants to a small set of familiar values, but instead have considered the materials that can in principle exist. Specific numerical results are presented in the following Section.

5. Numerical examples

A novel design for a narrowline bandpass filter is presented in Fig. 3. By allowing the unknown dielectric constants to span the range between 1 and 10 - a realistic assumption in the microwave - we have obtained a solution for a three-material single waveguide-grating transmission filter with a bandwidth of 0.7% of the central wavelength

of 3 cm. The geometry of the cell and illumination condition is reported in the figure, together with the obtained filter response. The prescribed response is a Lorentzian line approximated according to (10); for this particular case N=2, K=1 was sufficient to represent the Lorentzian with at least six digits of accuracy. As a results five design wavelengths were used to specify *RR**: 2.5, 2.75, 3, 3.25 and 3.5 cm. The residual was actually evaluated for a set of 103 wavelengths, not equally distributed in the range 2.5 - 3.5 cm, but rather having a denser distribution in a small region around the expected resonance (21 points in the range 2.98 - 3.02 cm). We took the population size to be 3000 with replacement of up to 300 at every generation and performed the calculations on the JPL Cray T3D. Gridding the cell with 21 x 7 points was sufficient to achieve convergence to the solution reported in the figure in about 150 iterations. For each iteration, the overall cost of replacement, i.e. the time necessary to evaluate the newly created strings at each iteration, was about 5 seconds using 64 processors.

As an example of a stopband filter, a response described by a fourth order Butterworth polynomial with bandwith of 8% of the center wavelength was input to the genetic algorithm as a prescribed reflectivity. A synthesized two-grating solution, the simplest realization with the smallest cell size which was found, is illustrated in Figure 4, with the obtained response contrasted with the desired one. Sixteen wavelengths were specified to represent the Butterworth curve according to (10), and the residual was calculated at 51 points. Both sets of points were uniformly distributed in the range of interest of 2.5-3.5 cm. The trial cell size was chosen to be 2x2.7 cm and was gridded with 10x14 points. A population size of 4000 with 10% replacement was chosen, and convergence was reached in about 300 generations. The calculation was performed on the Cray T3D using 128 processors in about 1 hour with a cost of replacement of about 13 sec.

Finally, to apply this method to a class of structures for which there are analytical solutions, we looked at the design of a five layer Fabry-Perot filter, and report the results in Figure 5. The design curve was obtained [17] with a forward scattering approach for a five

layer structure with thicknesses, from bottom to top, of 0.2, 0.5, 0.22, 0.5 and 0.2 cm. The correspondent original dielectric constants of the five materials were 6.13, 1, 6.13, 1, and 6.13. For use with our inverse approach, the design curve was approximated according to (10), using five wavelengths unequally distributed in the design range, specifically at 1.8, 1.9, 1.95, 1.986, and 2.1 cm. The 'cell periodicity' was taken to be 0.1 cm and the overall thickness was fixed at 1.62 cm. Note that the solution found by the GA is symmetric, with values of thicknesses and dielectric constants very close to those used to generate the design curve. In particular, no symmetry requirements were introduced as constraints. Since the reconstructed transmittivity is in very good agreement with the prescribed one, we can see that the sensitivity of the response to small variations in the design parameters (thicknesses and dielectric constants) is very small. This property is well known for Fabry-Perot filters.

6. Appendix

Applying Kumar's transformation to (4) it is obtained

$$E^s(x,z) = \frac{-\omega\mu}{4}\int_0^t dz' \int_0^{T_x} dx' J(x',z') \sum_m \Big[H_0^{(2)}\big(k\sqrt{(x-x'-mT_x)^2+(z-z')^2}\big)$$

$$- H_0^{(2)}\big(k\sqrt{(x-x'-mT_x)^2+(|z-z'|+\delta)^2}\big)\; e^{+jk_{x_0}mT_x}\Big]$$

$$- \frac{\omega\mu}{4}\int_0^t dz' \int_0^{T_x} dx' J(x',z') \sum_m H_0^{(2)}\big(k\sqrt{(x-x'-mT_x)^2+(|z-z'|+\delta)^2}\big)\; e^{+jk_{x_0}mT_x} \qquad \text{(A1)}$$

where δ is the shift away from the $|z-z'|$ axis. The first integral contains an integrable singularity, while the second can be transformed into a quickly convergent summation.

Use is made of the Poisson sum formula to convert the second integral in (A1) to a spectral domain summation. The Poisson sum formula is

$$\sum_{m=-\infty}^{\infty} f(\alpha m) = \frac{1}{\alpha} \sum_{m=-\infty}^{\infty} F\left(\frac{2m\pi}{\alpha} \right)$$

$$F(\omega) = \int_{-\infty}^{\infty} e^{j\omega z} f(z) dz$$

where we take

$$f(mT_x) = H_0^{(2)}(k\sqrt{(x-x'-mT_x)^2 + (|z-z'|+\delta)^2}) \; e^{jkx_0 mT_x}$$

and

$$F(k_x) = \frac{1}{2jk_z} \; e^{j(k_x+kx_0)(x-x')} e^{-jk_z(|z-z'|+\delta)}$$

The summation in the second integral of (A1) becomes

$$\frac{1}{T_x} \sum_{m=-\infty}^{\infty} \frac{1}{2jk_{z_m}} \; e^{j\left(\frac{2\pi m}{T_x}+kx_0\right)(x-x')} e^{-jk_{z_m}(|z-z'|+\delta)}$$

and the second integral is reduced to

$$\frac{\omega}{4} \sum_m \frac{1}{2jk_{z_m}} \Psi_m(x) \int_0^t dz' \tilde{J}_m(z') \; e^{-jk_{z_m}(|z-z'|+\delta)} \qquad \text{(A2)}$$

Then (A1) is given by

$$E^s(x,z) = \int_0^{T_x} dx' \int_0^t dz' J(x',z') \left[Z_m^p(x,z|x',z') - Z_m^p(x,z|x',z'+\delta) \right]$$

$$+ \sum \tilde{Z}_m \tilde{J}_m^{\pm} \Psi_m(x) \; e^{\mp jkz_m(z+\delta)} \qquad \text{(A3)}$$

where the - sign applies for $z > z'$ and the + sign for $z < z'$. The first integral in (A3) is the contribution from the singularity, whereas the summation pertains to the non singular part.

$$\tilde{J}_m^t = \int_0^{T_x} dx' \int_0^t dz' J(x',z') \Psi_m^*(x') \; e^{\pm jkz_m z'}$$

$$\tilde{Z}_m = -\frac{\omega\mu}{8jkz_m}$$

$$Z_m^p(x,z|x',z') = \frac{-\omega\mu}{4} \sum_m H_0^{(2)}(x,z|x',z') \; e^{jkx_0 mT_x}$$

Acknowlegements

The authors thank Dr. David Levine, formerly with Argonne National Laboratory and presently with the Boeing Company, for discussions on and assistance with use of PGAPACK. They are also indebted to Sorin Tibuleac, with the University of Texas at Arlington, TX, for discussions on dielectric waveguide - gratings filters and for providing independent calculations and verifications of some of the results presented here. Use of the Cray Supercomputers at the Jet Propulsion Laboratory, Pasadena, CA, is acknowledged. The research described here was performed at the Jet Propulsion Laboratory, under contract with the National Aeronautics and Space Administration.

References

[1] T. M. Habashy, L.M. Oristaglio, and A.T. de Hoop, " Simultaneous non linear reconstruction of two-dimensional permittivity and conductivity," *Radio Science,* vol. 29, pp. 1101-1118, Aug. 1994.

[2] R.E. Kleinman and P.M. van de Berg, " Two-dimensional location and shape reconstruction, *Radio Science,* vol. 29, pp. 1157-1169, Aug. 1994.

[3] D. Levine, "Users guide to the PGAPACK parallel genetic algorithm library," *Argonne National Laboratory - 95/18*, January 1996.

[4] R.L. Haupt, "Thinned arrays using genetic algorithms," *IEEE Trans. Antennas and Propagation,* vol. 42, pp.993-999, July 1994.

[5] E. Michielssen, J.-M. Sajer, S. Ranjithan, and R. Mittra, "Design of lightweight, broad-band microwave absorbers using genetic algorithms," *IEEE Trans. Antennas and Propagation,* vol. 41, pp. 1024-1030, June/July 1993.

[6] T. Eisenhammer, M. Lazarov, M. Leutbecher, U. Schoffel, and R. Sizmann," Optimization of interference filters with genetic algorithms applied to silver-based heat mirrors," *Applied Optics,* vol. 32, pp. 6310-6315, Nov. 1993.

[7] A. Boag, A. Boag, E. Michielssen, and R. Mittra, "Design of electrically loaded wire antennas using genetic algorithms," *IEEE Trans. Antennas and Propagation,* vol. 44, pp. 687-695, May 1996.

[8] E.E. Altshuler and D.S. Linden, "Design of a loaded monopole having hemispherical coverage using genetic algorithms, " *IEEE Trans. Antennas and Propagation,* vol. 45, pp. 1-4, Jan. 1997.

[9] A. John and R.H. Jansen, " Evolutionary generation of (M)MIC component shapes using 2.5D EM simulation and discrete genetic optimization, " *IEEE MTT-S Digest,* pp. 745-747, 1996.

[10] S. Chakrabarti, K.R. Demarest, and E.K. Miller, "An extended frequency-domain Prony's method for transfer function parameter estimation, " *Intl. J. Numerical Modeling:Electronic Networks, Devices and Fields,* vol. 6, pp.269-281, 1993.

[11] N. Amitay, V. Galindo and C. Wu, " Theory and analysis of phased array antennas, " New York, Wiley, pp. 310-313, 1972.

[12] R. Jorgenson and R. Mittra, " Efficient calculation of the free-space periodic Green's function, " *IEEE Trans. Antennas and Propagation,* vol. 38, pp. 633-642, May 1990.

[13] D. E. Goldberg, " Genetic Algorithms, " New York, Addison Wesley, 1989.

[14] S.S. Wang and R. Magnusson, "Multilayer waveguide-grating filters," *Applied Optics,* vol. 34, pp. 2414-2420, May 1995.

[15] R. Magnusson and S.S. Wang, "Transmission bandpass guided-mode resonance filters," *Applied Optics,* vol. 34, pp. 8106-8109, Dec. 1995.

[16] R. Magnusson, S.S. Wang, T.D. Black, and A. Sohn, " Resonance properties of dielectric waveguide gratings: theory and experiments at 4-18 GHz, " *IEEE Trans. Antennas and Propagation,* vol. 42, pp. 567-569, April 1994.

[17] S. Tibuleac, the University of Texas at Arlington, TX, private communication, Dec. 1996.

LIST OF FIGURES

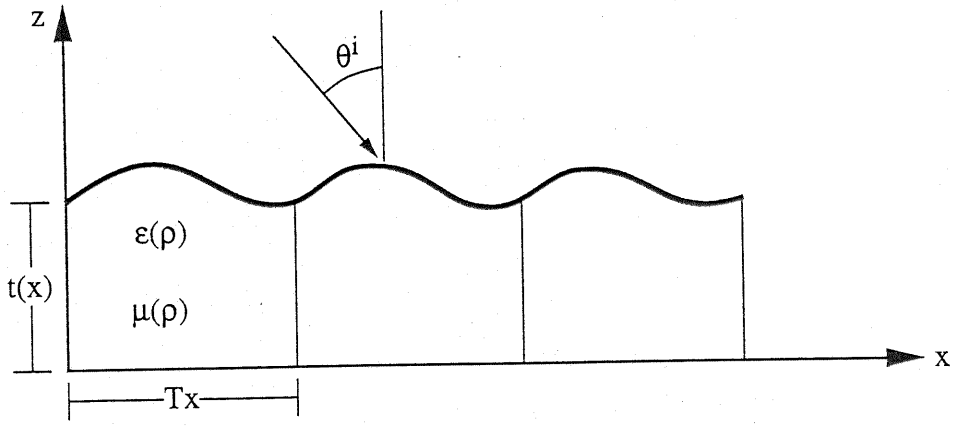

(a)

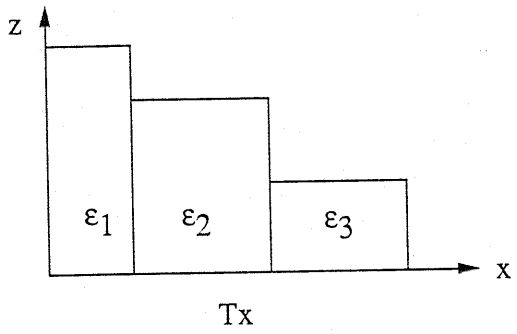

(b)

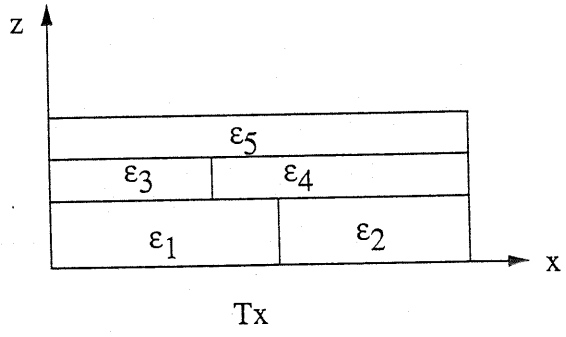

(c)

Fig. 1

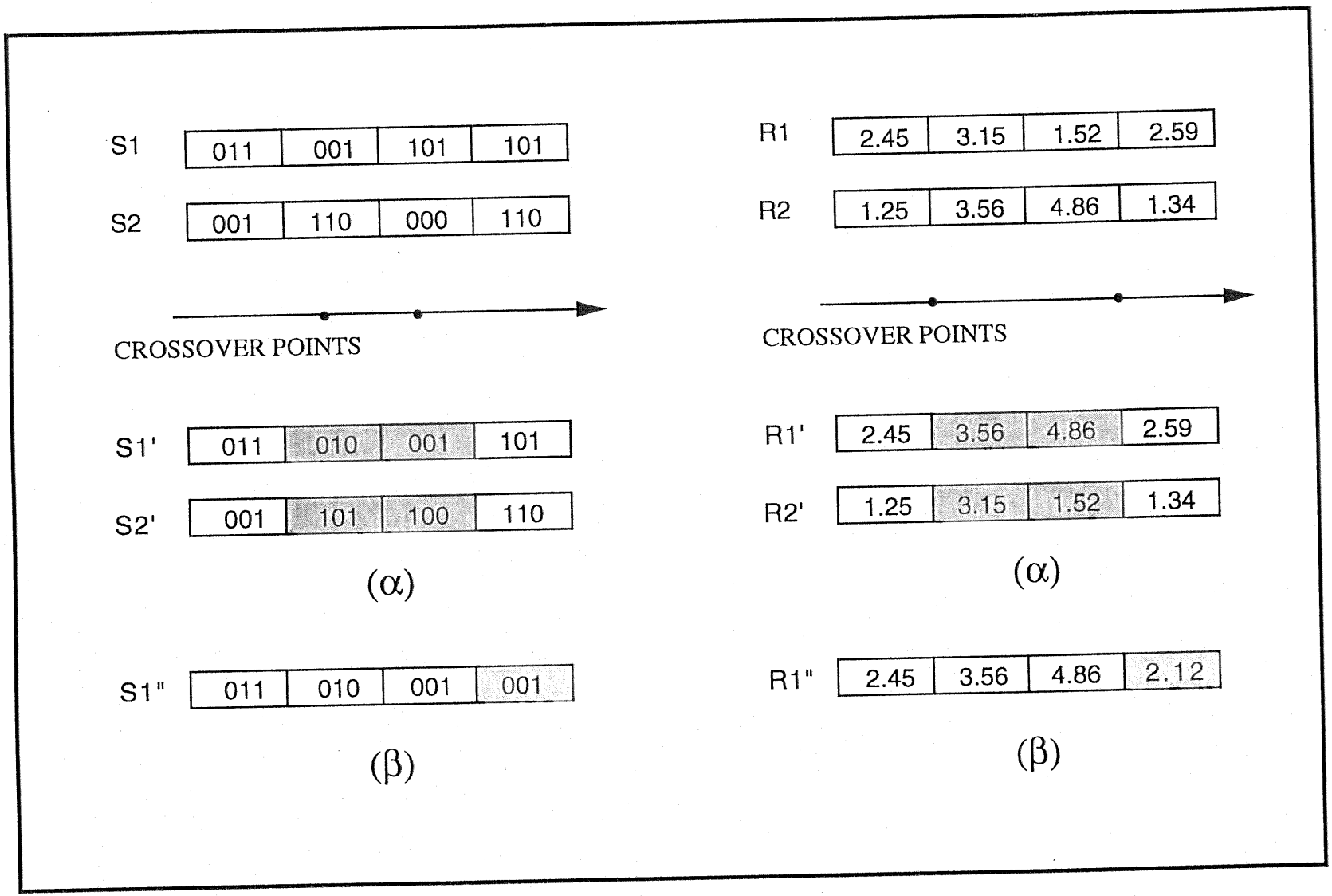
S1
011
001
101
101
S2
001
110
000
110
CROSSOVER POINTS
S1'
011
010
001
101
S2'
001
101
100
110
(α)
S1"
011
010
001
001
(β)
R1
2.45
3.15
1.52
2.59
R2
1.25
3.56
4.86
1.34
CROSSOVER POINTS
R1'
2.45
3.56
4.86
2.59
R2'
1.25
3.15
1.52
1.34
(α)
R1"
2.45
3.56
4.86
2.12
(β)

Fig. 8

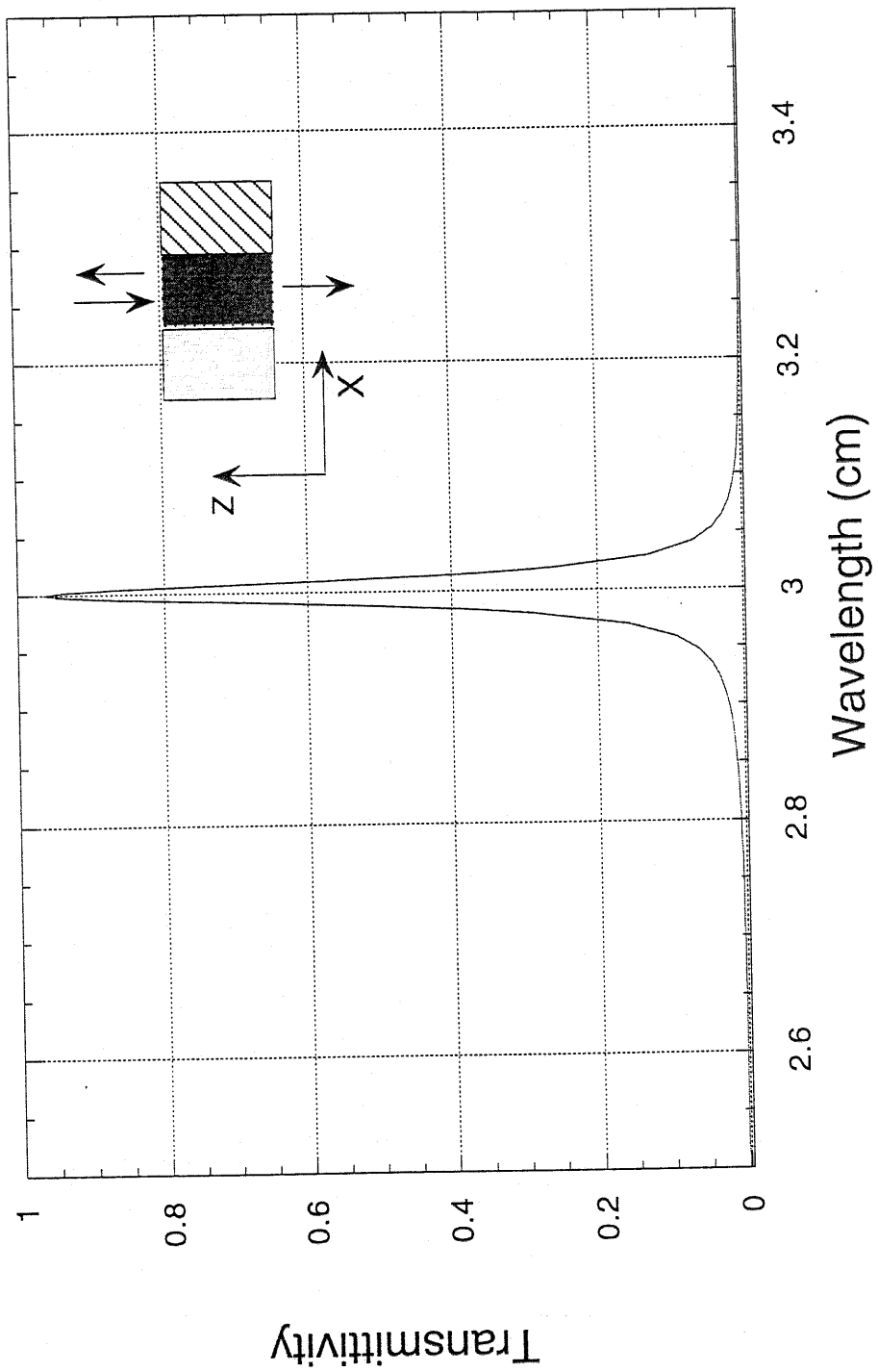

Fig. 3

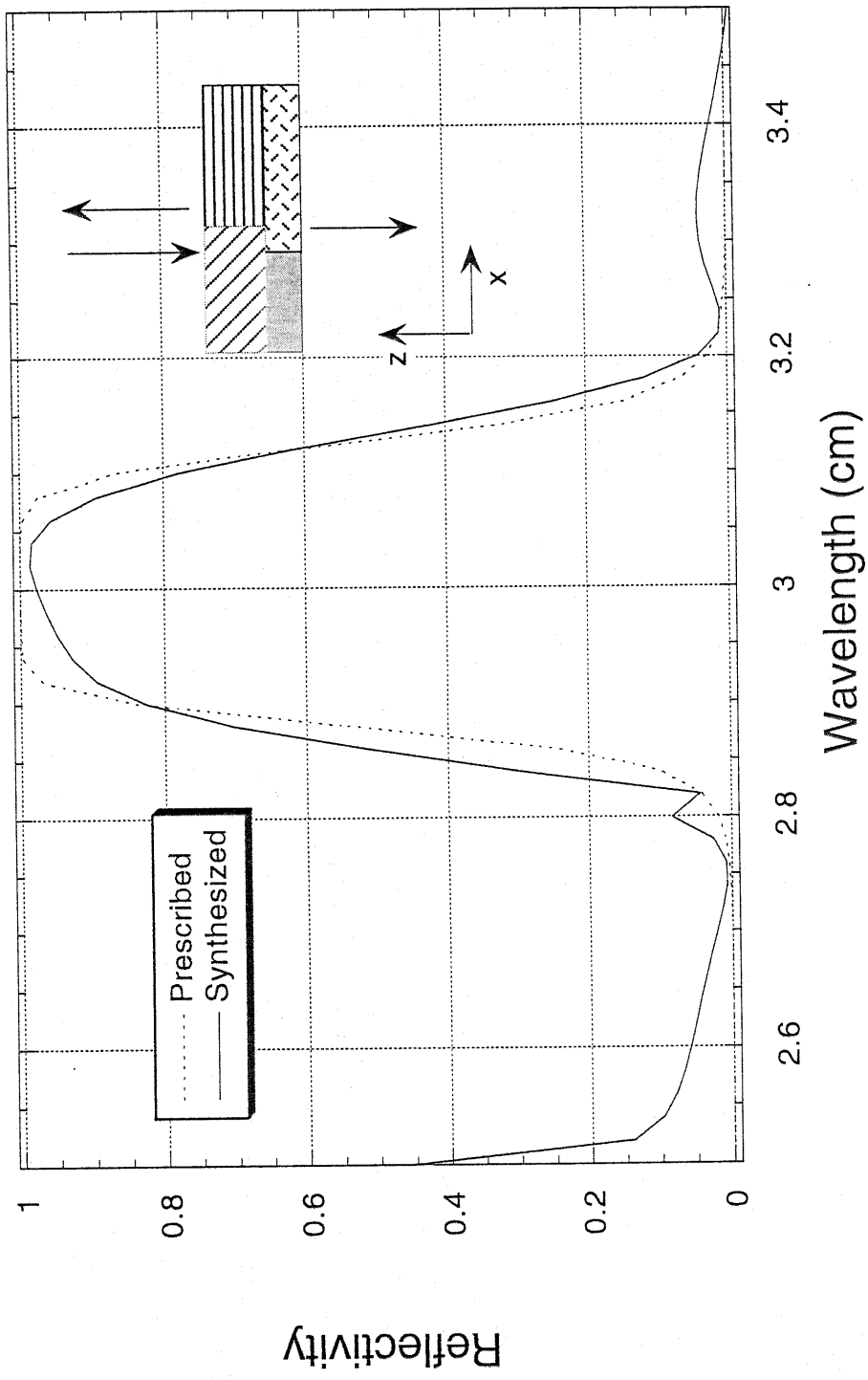
Reflectivity
1
0.8
0.6
0.4
0.2
0
2.6
2.8
3
3.2
3.4
Wavelength (cm)
Prescribed
Synthesized
z
x

Fig. 4

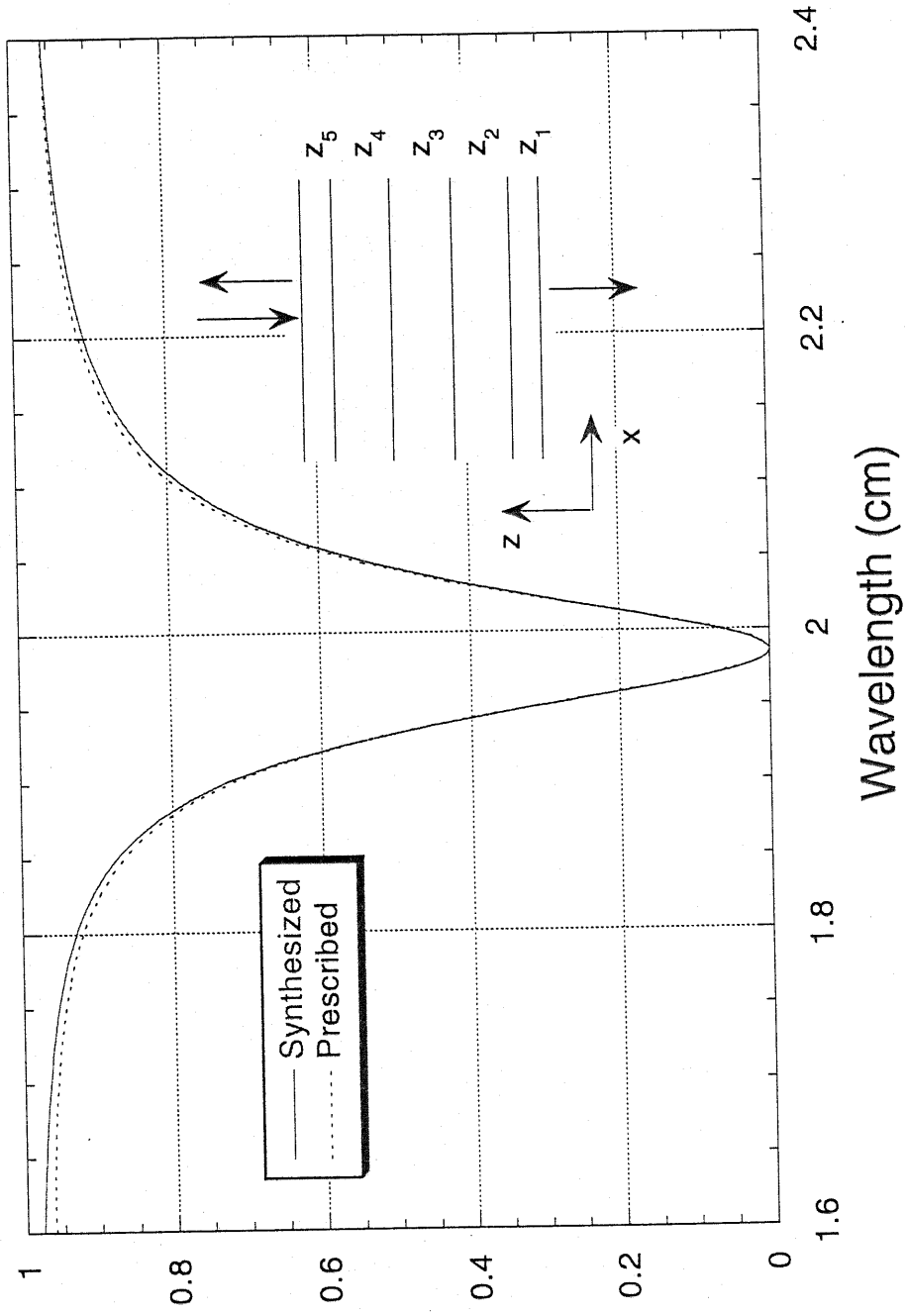
Reflectivity
Wavelength (cm)
1
0.8
0.6
0.4
0.2
0
1.6
1.8
2
2.2
2.4
Synthesized
Prescribed
z_5
z_4
z_3
z_2
z_1
z
x

Fig. 5